

RESILIENCE OF A TELECOMMUNICATIONS NETWORK SUBJECTED TO CORRELATED GEOGRAPHICAL FAILURES

DORA JIMÉNEZ¹ AND ABIGAIL MEDINA²



¹Universidad Adolfo Ibáñez. ²Universidad de Carabobo
dora.jimenez.a@edu.uai.cl, acolina6@uc.edu.ve

Abstract

Due to the COVID-19 pandemic, the way in which routine activities are carried out changed, taking a leading role telecommunications networks, it is important to evaluate their operation, service interruption and progressive deterioration, especially those generated by natural disasters, we have focused on earthquakes. Venezuela is a seismic country, being vulnerable to economic and human losses caused by this disaster. Many of the infrastructures that are used by both public and private institutions may not follow the current laws on earthquake-resistant structures. We seek to evaluate the damage by correlated geographic faults produced by earthquakes in a telecommunications network using probabilistic seismic risk analysis.

Keywords: reliability, seismic, simulation

1. INTRODUCTION

In the last three years due to the social isolation caused by the COVID-19 pandemic, the daily tasks, work and academic, have taken a turn driving more and more the need to access and have reliable telecommunications networks, since the activities that were traditionally executed in person, have been replaced by tools that allow to perform these tasks from home via the Internet, in addition to this, the trade could continue thanks to this. In a research carried out in 2021 by Valeria Castro in [1], it points out that the use of Internet increased globally by 70%, in fact it also shows a projection for 2025, and it is expected that this percentage will continue to increase. In [2] the methods currently used to assess individual seismic risk are based on many years of statistical data, they propose an end-to-end calculation-experimental approach to estimate possible losses and individual risk based on actual data on hazard, seismicity and earthquake resistance.

Due to the importance that telecommunication networks have taken, it is relevant to study the fragility of this, in order to know the possibility of partial or complete failure of the network, caused by typical or geographical failures, such as those generated by seismic events. Despite scientific and technological advances, human beings continue to be exposed to natural disasters, leaving in evidence the vulnerability of society to such events. It should be emphasized that these events cannot be avoided; however, thanks to globalization, it is possible to obtain information in real time about the predictions of these disasters (in case it is possible to predict them), or the strata caused by them, and this has been achieved thanks to the progress in telecommunications.

Venezuela throughout history has been affected by high intensity earthquakes, additionally most of the country's population is concentrated in the capital and northwest coast, being these some of the areas of greatest seismic threat [3], since along this region are the fault systems Boconó, San Sebastián and La Victoria, making the buildings that are located there more vulnerable to damage by such events.

Once the motivations for this research have been stated, the study of the vulnerability of the telecommunications network to earthquakes is focused on using as a case study a representation of the Venezuelan state communications network (Compañía Anónima Nacional Teléfonos de Venezuela, CANTV). A phased model is proposed through Monte Carlo simulation to determine the operability of the network components.

2. METHODOLOGY

The seismic hazard of Venezuela was identified in order to select the model that adapts to the geographic faults of the Venezuelan territory. John Douglas, in [4], proposes different functions for the study of ground motion in an earthquake, classifying them according to the zone and type of earthquake. Taking this into account, it was decided to use the equation to calculate the *SA* (spectral acceleration) described by Norman Abrahamson et al. (2016) and BC Hydro (2012) [5]. We follow the approach proposed by [6], where, using probabilistic seismic risk analysis, they evaluate the reliability of a telecommunications network in the event of earthquake failure in Chile, one of the most seismic countries in the world.

In the diagram 1 the processes executed in the simulation are visualized, applying a three-stage model, in the first one the characteristics of the earthquake itself necessary to generate the following stages are generated, some parameters of interest are the moment magnitude, depth and epicenter, subsequently an intensity measure describing the ground motion is generated, In this opportunity we work with the spectral acceleration (*SA*) and in the last one we calculate the fragility curves to obtain the probability that the components of the network suffer a specific level of damage (in this opportunity the levels of mild and extensive damage), which occurred given the spectral acceleration, as established by the HAZUS manual [7], this is achieved using Monte Carlo simulation, these steps are repeated *n* times, to finally calculate the marginal probability of failure of each component of the network.

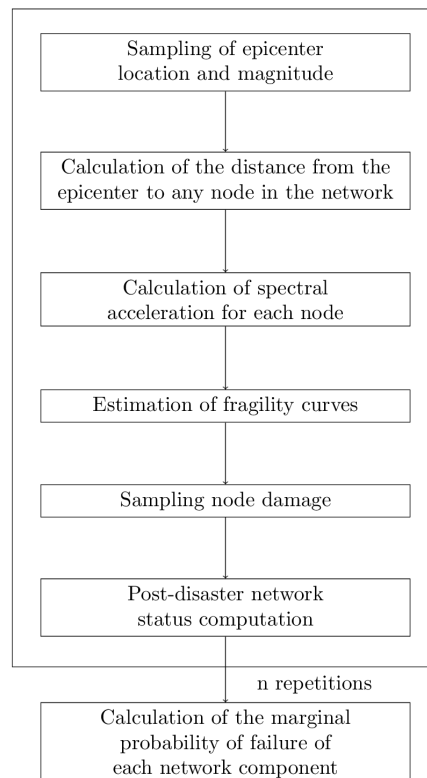


Figure 1: Flowchart of a generic Monte Carlo simulation run

The processes shown in the 1 diagram are presented in more detail below, starting with the model used to simulate ground motion.

2.1. Equation to predict ground motion

I know use the following equation of ground motion from Carlos Arteta et al. in [8], where SA_{ij} is the spectral acceleration at a given period; $f(M_i, r_{ij}, \theta)$ is the attenuation equation as a function of magnitude M , distance r and the model parameter vector Θ ; ϵ_{ij} is the error term for log j of event i and η_i is the random effect for event i .

$$\ln(SA_{ij}) = f(M_i, r_{ij}, \theta) + \eta_i + \epsilon_{ij} \quad (1)$$

The term θ_i represents between-event (or interevent) variations, while ϵ_{ij} represents within-event (or intra-event) variations. The residuals of η , ϵ are uncorrelated and are normally distributed with variances t^2 and f^2 , respectively. The total standard deviation of the ground motion model σ can be expressed as.

$$\sigma = \sqrt{\tau^2 + \sigma^2} \quad (2)$$

2.1.1 Functional form of the ground motion model

The mean of the model posited by Abrahamson (2016) and BC Hydro (2012) in [5], in future reference the abbreviation GMPE-Am2016 will be used for simplification of writing, is described in the following equation for interface and intraplate earthquakes:

$$\begin{aligned} \ln(SA) = & \theta_1 + \theta_4 \delta C_1 + (\theta_2 + \theta_{14} F_{event} + \theta_3 (M - 7.8)) \ln(R_{rup, hypo}) + (M - 6)) \\ & + C_4 \exp(\theta_9 + \theta_6 R_{rup, hypo} + \theta_{10} F_{event} + f_{mag}(M) + f_{depth}(R_{hypo}) F_{event} + \\ & + f_{FABA}(R_{rup, hypo}) + f_{site}(PGA_{1000}, V_{S30}) \end{aligned} \quad (3)$$

- SA is the spectral acceleration in gravity.
- M is the magnitude of the momentum.
- R is the event-dependent distance, e.g., R_{rup} the rupture distance for the interface and R_{hypo} the hypocentral distance for intraplate events.
- θ_j is the dependent event.
- $F_{event} = \begin{cases} 0 & \text{for interface events} \\ 1 & \text{for intra-board events} \end{cases}$
- $F_{FABA} = \begin{cases} 0 & \text{foreground or unknown sites} \\ 1 & \text{posterior arc sites} \end{cases}$

Model for magnitude scaling

$$f_{mag}(M) = \begin{cases} \theta_4 (M - (C_1 + \delta C_1)) + \theta_{13} (10 - M)^2 & \text{para } M \leq C_1 + \delta C_1 \\ \theta_5 (M - (C_1 + \delta C_1)) + \theta_{13} (10 - M)^2 & \text{otros casos} \end{cases} \quad (4)$$

Where $C_1 = 7.8$. The values of C_1 capture the epistemic uncertainty of magnitudes.

Model for scaling depth

$$f_{depth}(R_{hypo}) = \theta_{11} (\min(R_{hypo}, 120)) F_{event} \quad (5)$$

Model for scaling the fore/back arc:

$$f_{FABA}(R) = \begin{cases} \theta_7 + \theta_8 \ln\left(\frac{\max(R_{hypo}, 85)}{40}\right) F_{FABA} & \text{para } F_{event} = 1 \\ \theta_{15} + \theta_{16} \ln\left(\frac{\max(R_{rup}, 100)}{40}\right) F_{FABA} & \text{para } F_{event} = 0 \end{cases} \quad (6)$$

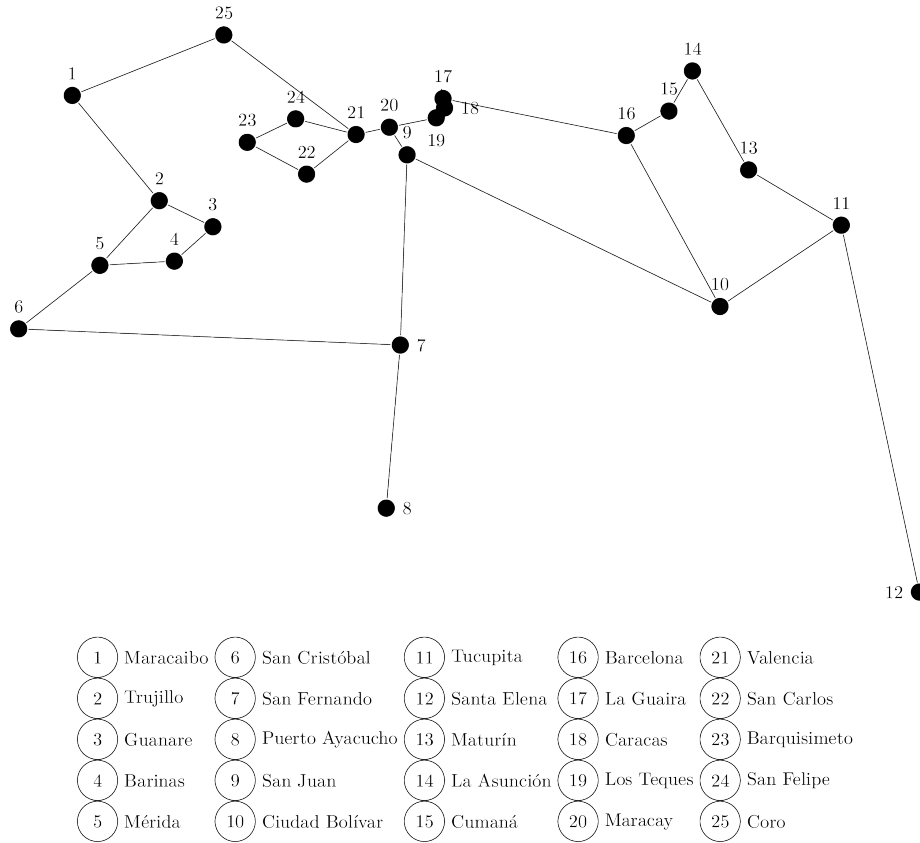


Figure 2: Venezuela's simplified telecommunications network graph

Model for scaling site response,

$$f_{site}(PGA_{1000}, V_{S30}) = \begin{cases} \theta_{12} \ln \frac{V_S^*}{V_{lin}} - b \ln PGA_{1000} + c + & \text{para } V_{S30} < V_{lin} \\ +b \ln PGA_{1000} + c \left(\frac{V_S^*}{V_{lin}} \right)^n & \\ \theta_{12} \ln \frac{V_S^*}{V_{lin}} - b \ln \frac{V_S^*}{V_{lin}} & \text{para } V_{S30} \geq V_{lin} \end{cases} \quad (7)$$

where PGA_{1000} = is the PGA median f $V_{S30} = 1000$ m/s and

$$V_S^* = \begin{cases} 1000 & \text{para } V_{S30} > 1000 \\ V_{S30} & \text{para } V_{S30} \leq 1000 \end{cases} \quad (8)$$

In this research for the calculation of the SA, the equation for the calculation of interface type earthquakes was used. Likewise, a model was proposed in which the different components of the Venezuelan telecommunications network are evaluated by damage levels. With the objective of calculating the marginal probability of failure for the nodes (cities of the network).

To calculate the probability of operability of each component it is necessary to use fragility curves, this corresponds to the graphical representation of the cumulative distribution function, also seen as the probability of reaching or exceeding a previously defined state of damage. In the case of earthquakes, such fragility curves have been defined in the HAZUS manual [7].

A telecommunication network can be viewed as a graph composed of nodes and arcs, the arcs connecting nodes to each other. The capitals of each state that make up the country and an additional city (Santa Elena de Uairén) were considered as the nodes of the network 2.

To perform the simulation of ground motion within an acceptable margin, with the GMPEAm-2016 model, a historical seismic base is necessary, for which it is essential to use a database that has a seismic research institution either national or international.

We use the data provided by the USGS (United States Geological Survey) Earth Explorer. Considering seismic events with magnitudes between 6 and 8, from 1900 to 2019, as shown in Figure 3.

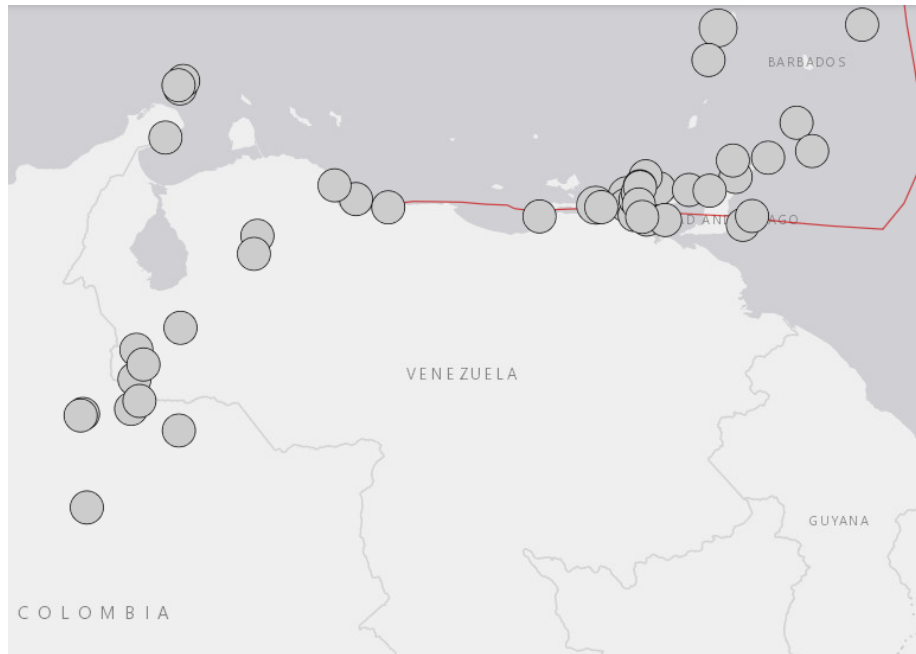


Figure 3: Geolocation of earthquakes between magnitude 6 and 8, image taken from [9]

Once the data was obtained, the ground motion simulation was performed, then the conditional probability was defined to evaluate the possibility of the component being operative after the earthquake. The probability of damage occurring, given that a displacement occurred in the component under study, is calculated using the equation for estimating fragility given by the HAZUS manual [7]. After obtaining the probability of failure, the state of the component was evaluated, for which a stochastic binary system is defined. Finally, the structure function for the Venezuelan telecommunications network was performed to calculate the marginal probability of each component. Finally, by quantifying the expected damage at each node, the corresponding analyses were performed to better understand the state of the network.

3. RESULTS

For this research, the RStudio program was used as a tool for the simulation, the calculations of the probabilities, as well as the graphs that are presented. The calculations and graphs were obtained by means of codes implemented in the aforementioned program using an Intel Core i3 – 3110M 1.4G laptop computer with 4GB of RAM memory. One thousand (1000) simulations were performed, a process that took 1.3399 seconds to execute, indicating that the associated computational cost is low.

For the mapping of the earthquakes, the data presented in Table 1, taken from [9], were used.

The locations used for the nodes are shown in the table below 2

For ground motion simulation, the GMPE-Am2016 model was implemented for interface type earthquakes, in the following Tables the parameters used for this model are presented.

Table 3, which was taken from [5], shows the coefficients to be used for the GMPE-Am2016 model, regardless of the period being worked with.

Table 1: Earthquakes (6 – 8 Mw), from 1900 to 2019, data obtained from [9]

Latitude	Longitude	Depth (Km)	Moment Magnitude
10.7731	-62.9019	146.82	7.3
6.7757	-72.9875	155	6.2
10.9048	-62.3150	63	6.0
10.7090	-67.9270	14	6.4
10.8760	-61.7560	53	6.1
11.1240	-62.5590	110.3	6.2
10.5980	-63.4860	19.9	7.0
11.1120	-60.8920	5	6.7
11.4120	-60.9420	45	6.1
5.0500	-72.9160	17.3	6.5
7.4140	-72.0330	11.6	6.0
10.2410	-60.7580	36.0	6.2
6.4700	-71.2100	20.3	6.1
10.9600	-68.3250	20.3	6.0
10.4020	-60.5870	56.2	6.7
10.5970	-62.9280	18.8	6.3
10.4190	-62.7640	40.0	6.1
10.0400	-69.7550	33.0	6.1
10.5630	-63.3820	34.0	6.1
9.4770	-72.5880	175.7	6.1
10.6970	-62.7480	103.4	6.5
10.5590	-67.3300	25.0	6.6
6.7470	-73.0320	161.2	6.8
10.3360	-62.5400	15.0	6.1
10.9420	-62.6680	15	6.0
10.8240	-62.7060	23.3	6.4
6.8680	-72.0950	25.0	6.6
8.3570	-71.1810	15.0	6.1
10.8630	-61.3740	49.0	6.1
7.0130	-71.9410	28.2	6.5
9.7100	-69.8190	15.0	6.4
10.5430	-64.4440	10.0	6.7
10.3620	-62.8040	20.0	6.3
11.8290	-71.4610	15	6.3
11.0000	-66.0000	0.0	7.7

Table 2: Geographic location of Venezuelan telecommunications network nodes

Number	City	Latitude	Longitude
1	Coro	11.4046	-69.6563
2	Valencia	10.1725	-67.9941
3	Maracay	10.2669	-67.6052
4	Los Teques	10.3486	-67.0344
5	Caracas	10.5002	-66.9191
6	La Guaira	10.6025	-66.9308
7	San Felipe	10.3400	-68.7452
8	Barquisimeto	10.0680	-69.3475
9	San Carlos	9.6600	-68.5811
10	San Juan de los Morros	9.9127	-67.3613
11	Ciudad Bolívar	8.0886	-63.5536
12	Barcelona	10.1450	-64.6783
13	Cumana	10.4322	-64.1833
14	La Asunción	11.0278	-63.8583
15	Maturín	9.7358	-63.1919
16	Tucupita	9.0697	-62.0456
17	San Fernando de Apure	7.8808	-67.4692
18	San Cristóbal	7.77194	-72.2264
19	Mérida	8.5700	-71.1808
20	Barinas	8.6231	-70.2372
21	Guanare	9.0378	-69.7289
22	Trujillo	9.3691	-70.4396
23	Maracaibo	10.645	-71.6131
24	Puerto Ayacucho	5.6625	-67.5828
25	Santa Elena de Uairén	4.6081	-61.1072

Table 3: Period-independent subduction model coefficients used in the regression analysis, Table taken from [5]

Coefficients	Value in all the periods
n	1.18
θ_3	0.1
θ_4	0.9
θ_5	0.0
θ_9	0.4
C_1	7.8
dC_1	0.2
C_4	10

Table 4: Regression coefficients for the median (units of g) of the ground motion model for interface earthquakes, taken from [5]

Coefficients	Value in all the PGA_{1000}	Value for the SA
Period	0.0000	0.2500
V_{lim}	865.1	654.3
b	-1.186	-2.381
θ_1	4.2203	5.0594
θ_2	-1.3500	-0.9940
θ_6	-0.0012	-1.3000
θ_7	1.988	2.8000
θ_6	-1.4200	0.0129
θ_8	0.9996	-1.3000
θ_{10}	3.1200	2.800
θ_{11}	0.0130	0.0129
θ_{12}	0.9800	2.4800
θ_{13}	-1.4200	-0.0172
θ_{15}	0.9996	1.1600
θ_{16}	-1.0000	-1.1700

In Table 4, the coefficients that depend on the period are shown, being equal to 0 used for the calculation of the PGA_{1000} and equal to 0.25 for the calculation of the SA.

Since the spectral acceleration was calculated for interface earthquakes, the coefficient θ_{14} has been omitted, since it is not necessary for this type of telluric movement. The value of V_{S30} used corresponds to [200,850], taking into consideration the works of Escobar et al. in [10] and [11], that of Morales and several authors in [12], and that of Acosta together with other authors in [13].

For the fragility curves, the following parameters presented in Table 5, selected from the HAZUS Manual [7] for reinforced concrete buildings (C2L), since the main CANTV telecommunications network exchanges are of this type of structures, two levels of damage were taken into consideration, slight and extensive, the first refers to cracks in the surfaces of the walls or small detachments of the concrete in some places, while the second is when most of the walls have exceeded their creep capacity, thus indicating cracks that go through the wall, extensive spalling around the cracks and wall reinforcement visibly bent or rotation of narrow walls with inadequate foundations, and partial collapse of the walls, the units are given in inches, so the corresponding conversion must be made, taking into account that the spectral acceleration is given in g .

Table 5: Structural parameters of the fragility curve

	Displacement Spectral (Inches)	
	Slight	Extended
$\bar{S}_{d,ds}$	0.72	1.04
β_{ds}	3.55	0.99

An Unif [0,1] was sampled to evaluate the state of the network components, i.e., whether there was damage or not, for which a dynamic binary system was established, taking the number one (1) to indicate that damage actually occurred in the node, and zero (0) for the opposite scenario. Once the thousands (1000) repetitions had been carried out, the marginal probability of each node receiving a slight or extensive level of damage was calculated. The following results were

obtained:

In Figures 4(a) and 4(b), the horizontal axis corresponds to the numbering assigned in the network for each city (see Figure 2 or Table 2), and the vertical axis to the number of times a failure occurred.

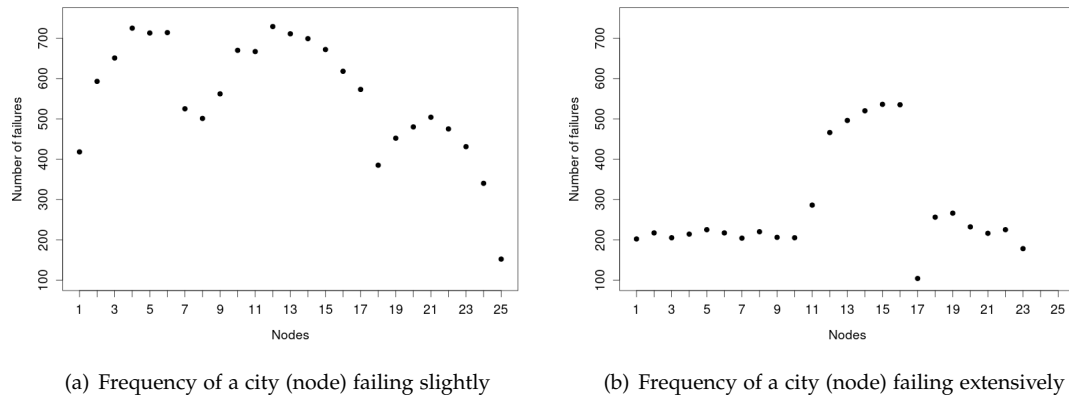


Figure 4: Frequency of occurrence of failure per damage level at each node

In Figures 4(a) and 4(b) three facts are observed, the first is that it is more frequent that a node receives a slight damage, as opposed to one of extensive level, second is that in Figure 4(a) the nodes that were damaged more than 600 times, were those corresponding to the following cities: Valencia (2), Maracay (3), Los Teques (4), Caracas (5), La Guaira (6), San Felipe (7), San Juan de los Morros (10), Ciudad Bolivar (11), Barcelona (12), Cumana (13), La Asunción (14) and Maturin (15), Los Teques and Barcelona being the two most recurrent nodes to receive slight damage, and close to 600 are San Carlos (9), Tucupita (16) and San Fernando de Apure (17), finally, in Figure 4(b) shows that La Asunción, Maturín and Tucupita received more than 500 times extensive damage, Barcelona and Cumaná between 400 and 500 times. Thus obtaining the probabilities presented in Figure 5, again the horizontal axis corresponds to the nodes, while the vertical axis in these graphs corresponds to the probability of failure.

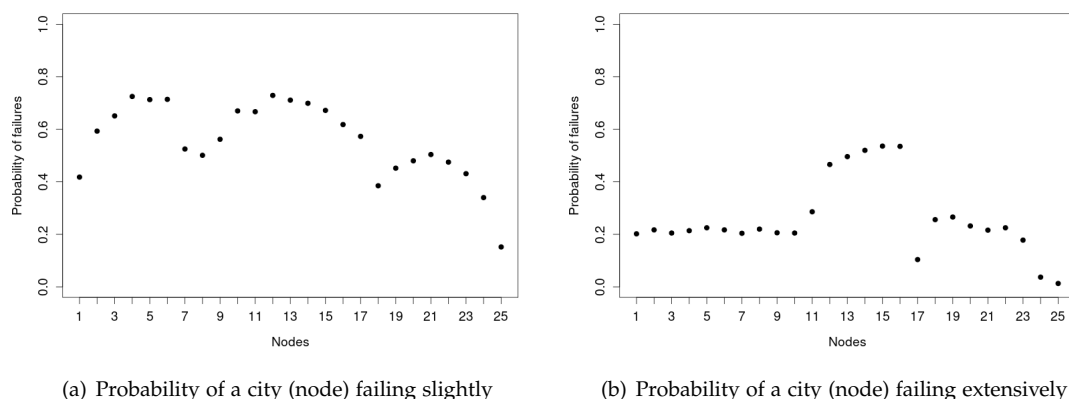


Figure 5: Probabilities of failure per damage level at each node

When comparing 5(a) and 5(b), with the geolocation of the earthquakes shown in the map 3, a geographical correlation is evidenced in which the nodes that have greater probability of

suffering damage, whether slight or extensive, are those that are closer to the areas with greater seismic activity; since the nodes that are observed in the graph 5(a) with a probability greater than 0.6 are mostly belonging to the capital, central and eastern regions of the country, and it is precisely these regions or near them that a greater number of earthquakes occur due to the system of active faults Boconó (Los Andes), San Sebastián (north-central Venezuela), and El Pilar (northeast of the country), their locations can be seen in the image 6.

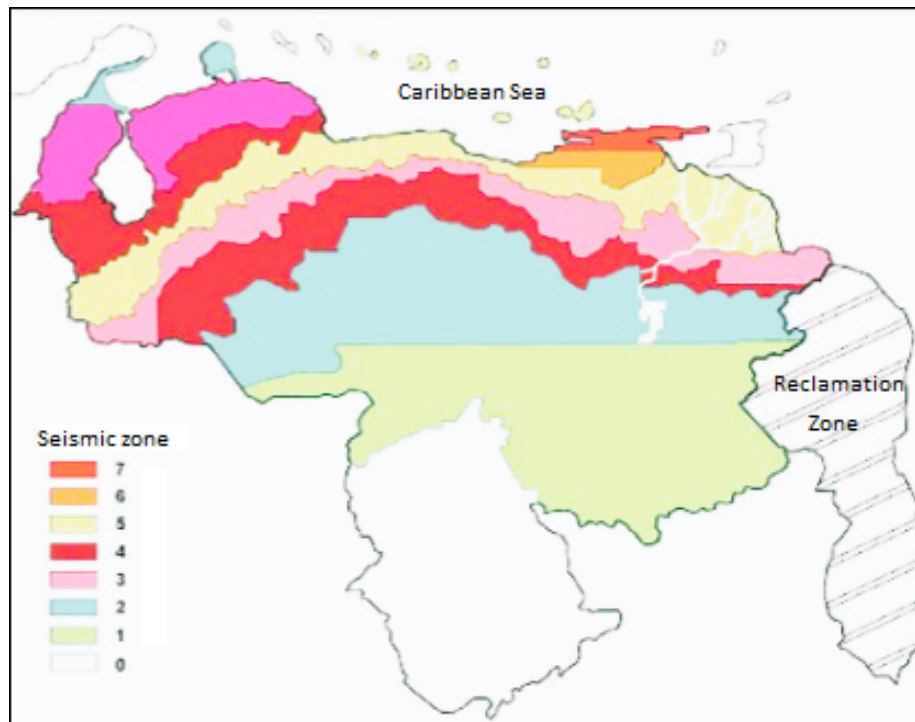


Figure 6: Seismic zonation map of Venezuela

The nodes with a probability of extensive damage greater than 0.5, shown in Figure 5(b), are those corresponding to La Asunción Maturín and Tucupita, which are located in one of the high seismic hazard zones (indicated by the orange color), as shown in the map 6. This correlation is also observed when analyzing the nodes with lower probability of damage in the two different levels, being the most notorious the Santa Elena de Uairén node (25) which has a slight probability of damage equal to 0.152, located in a zone of low seismic hazard (green color); and a probability of extensive damage to 0.013, another node with a low probability of extensive damage is Puerto Ayacucho (24) with an occurrence equal to 0.037, and also located in a zone with seismic hazard similar to the previous one.

In the graph 7 the fragility curves for C2L buildings are shown, where the blue curve represents the probability that given a spectral acceleration the mild damage state is exceeded or reached, and the green one for extensive damage, on the horizontal axis the SA is expressed and on the horizontal axis the conditional probability that a damage state is exceeded given the intensity measure, in this case the SA. It is clear from this graph that slight damage has a higher probability of occurrence than extensive damage, which is the expected result.

4. CONCLUSIONS

A study was carried out on the operability of the components of the Venezuelan telecommunications network when affected by earthquakes. For this purpose, a model was implemented to calculate the spectral acceleration in order to perform a simulation of ground motion, taking into consideration the characteristics of the infrastructure and geography, and thus be able to evaluate

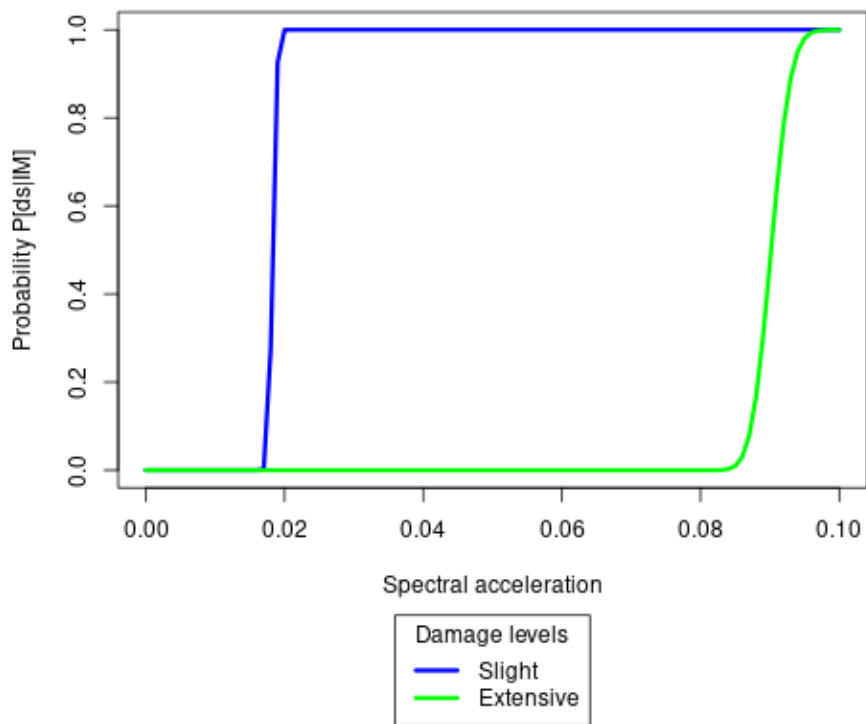


Figure 7: Fragility curves for mild and extensive damage levels

the probability of exceeding a previously defined damage state (in this opportunity, light and extended damage were established), and thus obtain the marginal probability of each component receiving a level of damage.

The network was tested with specific earthquakes (6 – 8 Mw), obtaining as a result that the probability that the nodes of the network suffer a slight or extensive level of damage is geographically related to the location of the earthquakes, so they have a higher probability of slight damage compared to extensive damage.

It is suggested to consider possible damage to the network arcs, since it is known that earthquakes can cause damage to these components. This study represents a novel proof of concept for the Venezuelan case and serves as a starting point for further studies.

ACKNOWLEDGMENT

This research received no specific grant from any funding agency in the public, commercial, or not-for-profit sectors.

REFERENCES

- [1] Valeria Castro Obando. Regulación, infraestructura y telecomunicaciones en la crisis del covid-19.
- [2] Gennadiy Nigmatov, Andrey Savinov, and Temir Nigmatov. Assessment of individual seismic risk for the population, taking into account the actual seismic resistance of buildings and the seismicity of soils. *Reliability: Theory & Applications*, 17(SI 4 (70)):172–179, 2022.
- [3] Omar Pérez. Sismicidad y tectónica en Venezuela y áreas vecinas, 1998.
- [4] Jhon Douglas. Ground motion prediction equations 1964–2021, May 2021.
- [5] Norman Abrahamson, Nicholas Gregor, and Kofi Addo. BC Hydro ground motion prediction equations for subduction earthquakes, 2016.
- [6] Dora Jiménez, Javiera Barrera, and Héctor Cancela. Communication network reliability under geographically correlated failures using probabilistic seismic hazard analysis. *IEEE Access*, 2023. Accepted.
- [7] MH HAZUS. Multi-hazard loss estimation methodology: earthquake model, 2003.
- [8] Carlos Arteta, Cesar Pajaro, Vicente Mercado, Julián Montejo, Mónica Arcila, and Norman Abrahamson. Ground-motion model for subduction earthquakes in northern South America. *Earthquake Spectra*, 37(4):2419–2452, 2021.
- [9] Usgs.Gov. Latest earthquakes. <https://earthquake.usgs.gov/>.
- [10] Marysol Mijares, Michael Schmitz, Javier Sanchez, and Freddy Rondón. Estudio del parametro VS30 mediante iMASW en la ciudad de Valencia.
- [11] Víctor Escobar, Michael Schmitz, Javier Sánchez, and Freddy Rondón. Estudio de interferometría del análisis multicanal de ondas superficiales (iMASW) para VS30 en Maracay study of interferometric analysis of surface waves (iMASW) for VS30 in Maracay.
- [12] Cecilio Morales, Julio Hernández, Michael Schmitz, Víctor Cano, and Mauricio Tagliaferro. Velocidades promedio de ondas de corte en los primeros 30 m de profundidad (V_{s30}), inferidas a partir del relieve en el área metropolitana de Caracas. *Revista de la Facultad de Ingeniería Universidad Central de Venezuela*, 26(2):161–168, 2011.
- [13] Rafael Acosta, Freddy Rondón, and Michael Schmitz. Mapa de VS30 de Carúpano a partir de la topografía v_{s30} map of Carúpano based on the analysis of the topography.